processes

MDPI

Article

Simulation Study of Wellbore Three-Phase Flow After Gas Invasion in Large-Displacement Wells Drilled in Seabed Hydrates

Bin Li [1], Jianwei Di [2], Xiaodong Wu [2], Wenhao Gong [3], Jinxing Wang [3], Song Deng [3] and Chaowei Li [3,*]

[1] Guangzhou Marine Geological Survey, Guangzhou 511458, China
[2] Engineering Design Institute, CNPC Offshore Engineering Co., Ltd., Beijing 100028, China; dijw.cpoe@cnpc.com.cn (J.D.)
[3] School of Petroleum and Natural Gas Engineering, Changzhou University, Changzhou 213164, China
* Correspondence: chw25@163.com

Abstract: During the drilling of natural gas hydrate reservoirs, gas invasion may occur, which has an adverse impact on the upward return process of cuttings and the control of bottom-hole pressure. A multiphase fluid CFD simulation method based on the Eulerian model was optimized. With the help of Fluent 23R1 software, simulations of the three-phase flow of drilling fluid–cuttings–invaded gas in the vertical section, build-up section, and horizontal section of the complex annulus multiphase flow in the hydrate drilling wellbore based on particle dynamics were carried out. The characteristics of multiphase flow in the wellbore after gas invasion were revealed, and the impacts of gas invasion on the deposition and migration of cuttings and the control of bottom-hole pressure were analyzed. The research shows that after gas invades the wellbore, it has little impact on the upward return of cuttings in the build-up section. However, in the vertical and horizontal sections, with the increase in the flow rate of the invaded gas, the slip and upward return of cuttings are promoted. The gas invasion velocity has a more significant impact on the cutting migration in different well sections compared to the gas invasion volume fraction. A faster invasion velocity accelerates the upward return of cuttings in the wellbore annulus. When gas invasion occurs, it has little impact on the pressure in the build-up section, decreases the pressure gradient in the vertical section, and increases the pressure gradient in the horizontal section. At the same time, there is a high linear correlation between the pressure gradient in each well section and the density of water-based drilling fluid. By reasonably controlling the density of drilling fluid according to the gas volume fraction detected at the wellhead, the aggravation of gas invasion can be significantly prevented. The research methods and calculation results are helpful in providing a reference for the subsequent drilling process of hydrate reservoirs.

Keywords: hydrate drilling; gas invasion; multiphase flow; cutting return; bottom-hole pressure control

check for updates

Academic Editor: Qingbang Meng

Received: 30 November 2024
Revised: 20 January 2025
Accepted: 6 February 2025
Published: 7 February 2025

Citation: Li, B.; Di, J.; Wu, X.; Gong, W.; Wang, J.; Deng, S.; Li, C. Simulation Study of Wellbore Three-Phase Flow After Gas Invasion in Large-Displacement Wells Drilled in Seabed Hydrates. *Processes* **2025**, *13*, 455. https://doi.org/10.3390/pr13020455

Copyright: © 2025 by the authors. Licensee MDPI, Basel, Switzerland. This article is an open access article distributed under the terms and conditions of the Creative Commons Attribution (CC BY) license (https://creativecommons.org/licenses/by/4.0/).

1. Introduction

The seabed of the South China Sea is rich in hydrate resources, regarded as an important clean energy alternative to traditional oil and gas resources. Between 2017 and 2020, China successfully conducted two rounds of a total of four hydrate extraction tests in the Shenhu area of the South China Sea [1], positioning the country at the forefront of global hydrate extraction technology. During the second hydrate extraction led by the China

Geological Survey, horizontal well development technology was employed, significantly increasing the contact area between the wellbore and the hydrate reservoir. However, when drilling into the hydrate reservoir, gas intrusion into the wellbore occurs, forming a three-phase flow state of drilling fluid, cuttings, and intruding gas. This state adversely affects the cutting return process and the control of bottom-hole pressure [2].

Currently, Lv et al. [3] utilized the Euler model to simulate the gas–liquid–solid three-phase flow characteristics of hydrate slurry under high-pressure conditions, analyzing the effects of inlet velocity, hydrate volume fraction, liquid-phase viscosity, and pipe diameter on the flow. The results indicate that pipe diameter significantly affects pressure drop, while liquid-phase viscosity influences particle aggregation. Hydrates accumulate at bends and exhibit symmetrical distribution. Pang et al. [4] studied the transport of multi-sized cuttings in horizontal wellbores with non-Newtonian fluids, modeling the cutting flow regime and its interaction with drilling fluid turbulence using particle flow dynamics theory. The study found that the non-uniformity of non-Newtonian fluid viscosity and particle settling led to complex stratified flow regimes, affecting cutting concentration and velocity distribution. Wei et al. [5] established a kinetic model of temperature, pressure, and hydrate decomposition, using numerical simulation to explore the impact of different parameters on multiphase flow behavior. The study revealed that with hydrate decomposition and flow changes, the temperature and pressure in the annulus exhibit significant fluctuations, potentially leading to well control safety issues. Epelle et al. [6] employed a two-fluid Euler–Euler multiphase flow model for simulation. The study showed that mud rheology, particle sphericity, and particle size are crucial for cutting removal, especially in the lower annular region of upward bends, where particle deposition is evident. Salubi et al. [7] evaluated the transport mechanism of cuttings under different flow regimes through experiments and mathematical modeling, finding that fluid flow regime and drilling fluid flow rate are the main influencing factors. However, during seabed hydrate drilling, the shallow seabed formation strength is low, with fast drilling speed and high displacement, leading to high cutting concentration in the wellbore. If gas intrusion is severe, the three-phase flow state in the wellbore becomes more complex. To date, most of the simulations of multiphase flow in the wellbore for hydrates focus on the settlement state of solid–liquid two-phase flow cuttings. However, for the problem of well killing caused by gas intrusion into the wellbore during the drilling process, there are currently few simulation studies.

In this paper, aiming at the problem of gas intrusion during subsea hydrate drilling, a multiphase fluid CFD simulation method based on the Eulerian model was optimized. With the help of Fluent 23R1 software, a three-phase flow simulation in the hydrate drilling wellbore was carried out, which can accurately analyze the characteristics of multiphase flow in the wellbore after gas intrusion, as well as the impact of gas intrusion on the deposition and migration of cuttings and the control of bottom-hole pressure.

2. Drilling Fluid–Cuttings–Intruding Gas Three-Phase Flow Simulation Method

2.1. Simplified Model of a Real-Scale Wellbore and Well Section

Figure 1 shows the well depth structure diagram of the second hydrate extraction. The wellbore structure data of the extraction well are shown in Table 1. The kickoff point is at a true vertical depth of 1455 m, and the inclination angle of the stabilized section of the wellbore is assumed to be 65°.

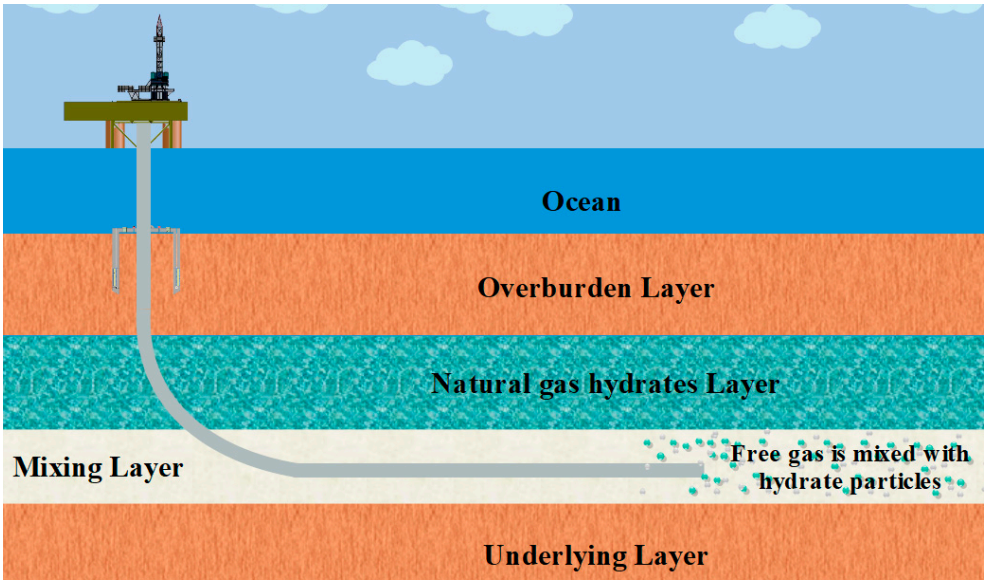


Figure 1. Hydrate reservoir schematic diagram [8].

Table 1. Simulation data table.

Drilling Fluid			Cuttings	
Upward Return Velocity	0.77 m/s		Density	1800 kg/m^3
Density	1100 kg/m^3		Volume Fraction of Cuttings	0.1
Viscosity	0.33 kg/(m·s)		Diameter	15 μm
Gas Phase			Geometrical Parameters	
Density	0.6679 kg/m^3		Drill Rod Diameter	0.14923 m
Viscosity	0.00001087 kg/(m·s)		Wellbore Diameter	0.31115 m
Infiltration Amount	Volume Fraction of Gas Intrusion	0.1, 0.3, 0.5, and 0.7	Simulated Wellbore Section Length	10 m
	Gas Intrusion Velocity	0.5 m/s, 1 m/s, 1.5 m/s, and 2 m/s		

Focusing on the horizontal wellbore of the second hydrate extraction [9], based on the horizontal wellbore structure (including the vertical section, stabilized section, and horizontal section), a numerical simulation model of wellbore flow in the vertical, stabilized, and horizontal sections was established to study the gas–liquid–solid flow patterns within the wellbore during gas intrusion in shallow hydrate drilling. A 12-1/4 in wellbore and a 5-7/8 in drill pipe were used. According to the well depth structure diagram of the horizontal well for the second hydrate test production and the schematic diagram of the hydrate reservoir [9], the wellbore of the second hydrate test production is mainly divided into three sections: the vertical section, the constant-inclination section, and the horizontal section. A 10 m long wellbore at a vertical distance of 1225.23 m from the wellhead is taken as the vertical section; a 10 m long wellbore at a vertical distance of 1455 m from the wellhead is taken as the constant-inclination section; a 10 m long wellbore at a vertical distance of 1490 m from the wellhead is taken as the horizontal section. Their detailed positions are shown in Figure 2. The vertical wellbore is described in Section A, the constant-inclination wellbore is described in Section B, and the horizontal wellbore is described in Section C. The deviation angle of the build-up section is 65°. The remaining engineering

parameters are shown in Table 1. By simulating the three wellbore sections with different characteristics, it is possible to reflect the states of different sections of the entire wellbore when the drilling fluid carries cuttings in the drilling process, as well as the pressure changes and the upward return states of cuttings in different wellbore sections after gas intrusion. This can comprehensively and accurately simulate the density of drilling fluid required for well killing in the subsequent process.

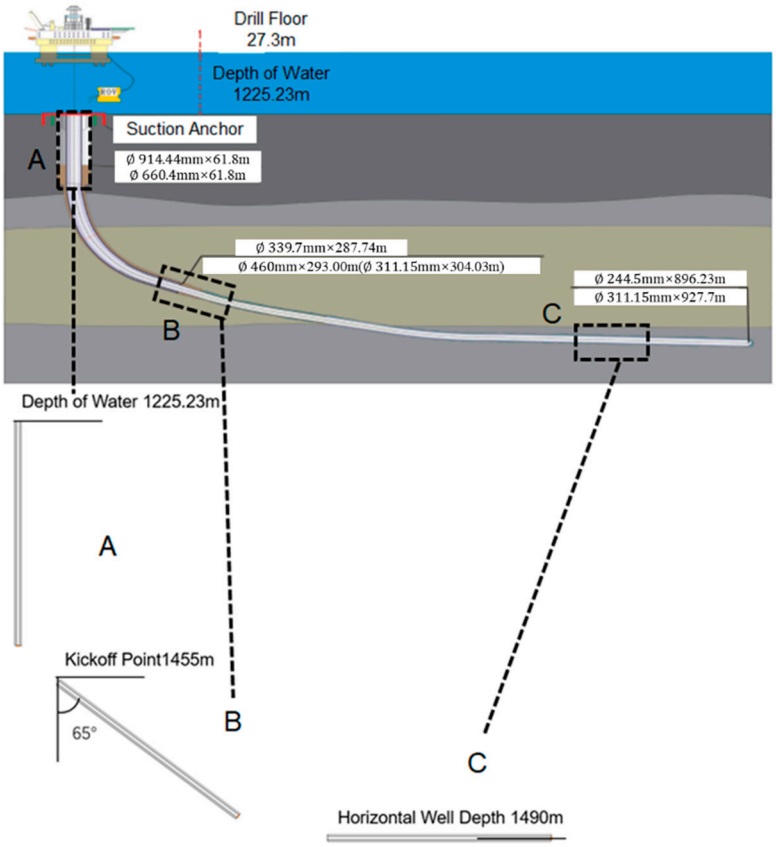


Figure 2. Geometry model of the vertical section, stable inclined section, and horizontal section of a horizontal well.

2.2. Mesh Generation Method and Grid Independence Verification

Mesh generation was performed for the established vertical, stabilized, and horizontal section models. Since the geometric models are simple concentric annular pipes, each being 10 m in length, the mesh generation is similar, utilizing structured hexahedral meshing through ICEM, as shown in Figure 3.

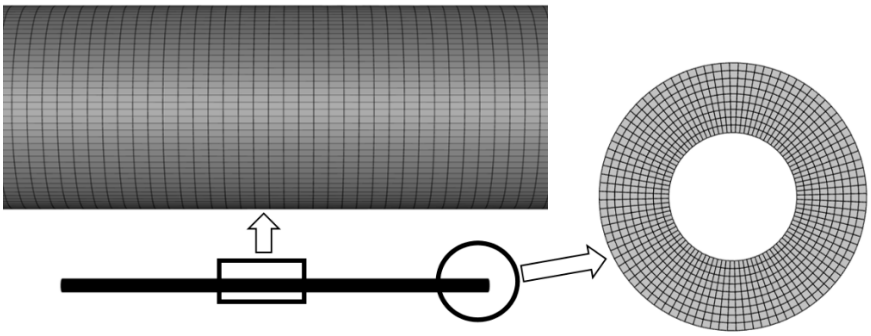


Figure 3. Wellbore mesh partitioning.

Taking the wellhead at the bottom of the vertical section as the inlet, the annular return velocity of the liquid-phase drilling fluid as 0.77 m/s (as shown in Table 1), the

gas-phase intrusion velocity as 0.5 m/s, the volume fraction as 0.2, and the solid-phase cuttings particles with a volume fraction of 0.1 as an example, a simulation experiment was carried out. The fluid velocity at the middle position of the vertical section at the end of the simulation calculation was recorded. The simulation results are shown in Figure 4. When the number of meshes reaches 157,436, further increasing the number of meshes does not result in significant differences in the simulation results. Therefore, the model corresponding to this number of meshes was adopted for fluid numerical simulation. For the build-up section B and the horizontal section C, the same mesh generation method of the above-mentioned mesh model was used, and fluid simulations were also conducted.

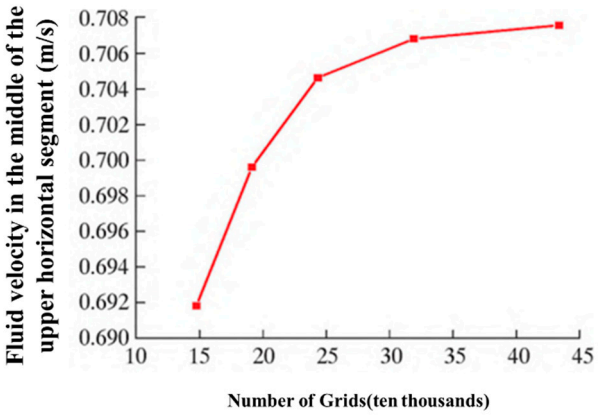


Figure 4. Mesh independence verification.

2.3. Multiphase Flow Parameter Optimization and Model Setup

The Phase-Coupled SIMPLE method is optimally used to handle the coupling relationship between pressure and velocity. This method effectively addresses coupling issues in fluid dynamics [10]. During spatial discretization, the Least-Squares Cell-Based method is employed to enhance the accuracy and stability of numerical calculations [11]. To ensure second-order accuracy of the pressure field and reduce errors, the pressure parameter is set to Second Order [12]. The momentum parameter uses the First Order Upwind method to avoid numerical oscillations [13]. During the calculation process, to effectively control fluid compressibility and improve computational accuracy, the volume fraction is set to Compressive, while the turbulent kinetic energy and turbulent dissipation rate use First Order Upwind [14]. The realizable k-epsilon turbulence model and scalable wall functions are selected to more accurately capture turbulence phenomena and have broader applicability [15,16]. The scalable wall function is suitable for the k-ε model, allowing better simulation of the flow in the boundary layer. This combination considers both the physical characteristics of turbulence and wall effects in the calculation, achieving more accurate results. The Euler model is used to simulate the gas–liquid–solid multiphase flow during gas intrusion in the drilling process [17,18]. Based on the Euler model, the velocity fields and temperature fields of each phase are solved separately, and the interaction between phases is modeled through the drag force, which can accurately track the interfaces between multiple fluids. Methane is selected as the gas-phase material, with a gas-phase viscosity of 0.017 mPa·s and a density of 0.6679 kg/m^3. The liquid phase is set as the drilling fluid, with a viscosity of 33 mPa·s and a density of 1040 kg/m^3. The solid phase consists of cutting particles from the hydrate reservoir, with a density of 1800 kg/m^3 and a cutting diameter of 15 μm. The boundary conditions of the simulation model are set as the velocity inlet and pressure outlet. The numerical simulation process is shown in Figure 5.

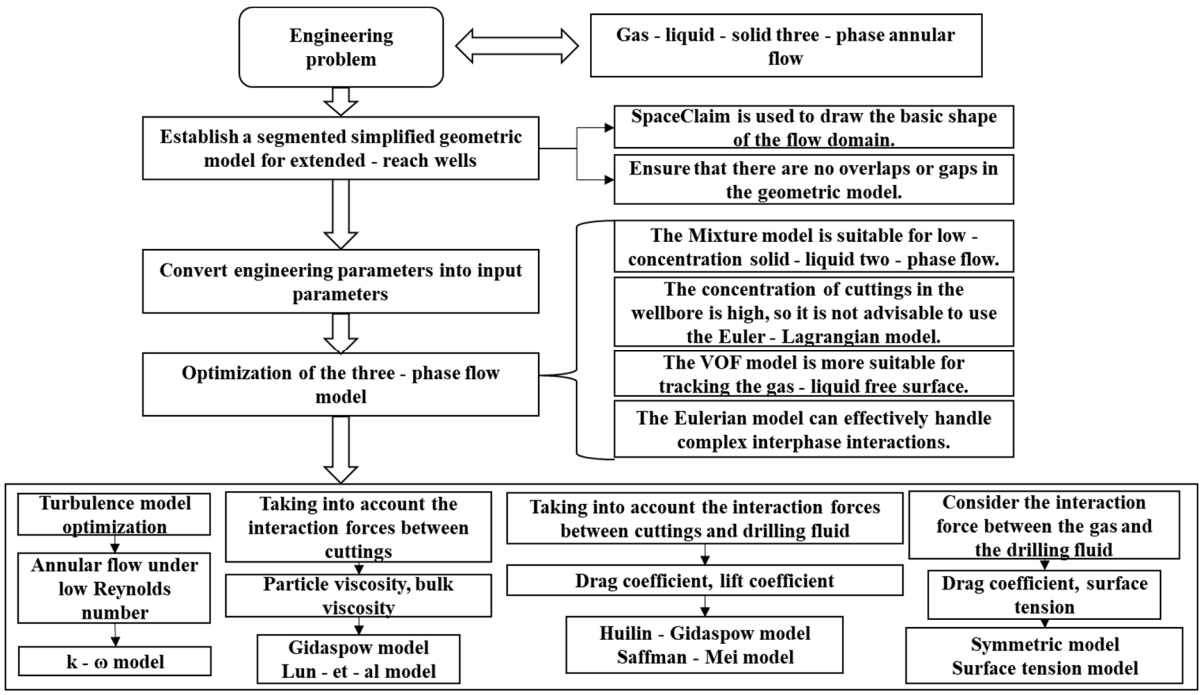


Figure 5. Numerical Simulation Process.

2.4. Model and Method Validation

A full-scale gas kick experiment is used to validate the multiphase flow behavior in the wellbore during free gas intrusion. For model validation, the experimental data from Rommetveit and Vefring [19] are used: in the experiment, the full-scale well depth is 2030 m, with a maximum inclination angle of 63°. During the first 660 s of the experiment, free gas is injected into the wellbore; after 660 s, the drilling pump is activated. Detailed information on the well structure and experimental procedures can be found in the study by Rommetveit and Vefring (1991).

Figure 6 shows a comparison of gas kick characteristics between the experimental data and the calculation results of the model in this paper, including bottom-hole pressure and outflow rate. During the gas invasion stage, the bottom-hole pressure drops first. This is mainly because the gas starts to enter the wellbore, breaking the original pressure equilibrium in the wellbore. Since the gas is lighter, its invasion will dilute the density of the fluid in the wellbore to a certain extent. According to the relationship between pressure and fluid density, the pressure decreases accordingly. At the same time, the entry of gas changes the flow state of the fluid in the wellbore, forming a local low-pressure area, which further promotes the decrease in the bottom-hole pressure. As the gas continues to invade, the bottom-hole pressure rises, and the gas–liquid mixing situation in the wellbore changes. The gas gradually accumulates and forms a gas column within a certain range, exerting an extrusion effect on the lower-part fluid, causing the bottom-hole pressure to rise back. In addition, during the gas–liquid mixing process, local fluid blockage may occur, hindering the smooth flow of the fluid, thus causing the pressure to increase. After that, due to the large influx of gas, the bottom-hole pressure drops significantly, making the flow state of the fluid in the wellbore extremely complex. The gas forms a large gas mass or gas layer, which breaks the continuity of the fluid, making it unable to transmit pressure effectively and reducing the pressure transmission efficiency. At the same time, the interaction between the gas, liquid, and solid phases intensifies, generating additional energy losses and further reducing the bottom-hole pressure. The results show that the two are basically consistent in quantity and trend, with a difference of less than 10%.

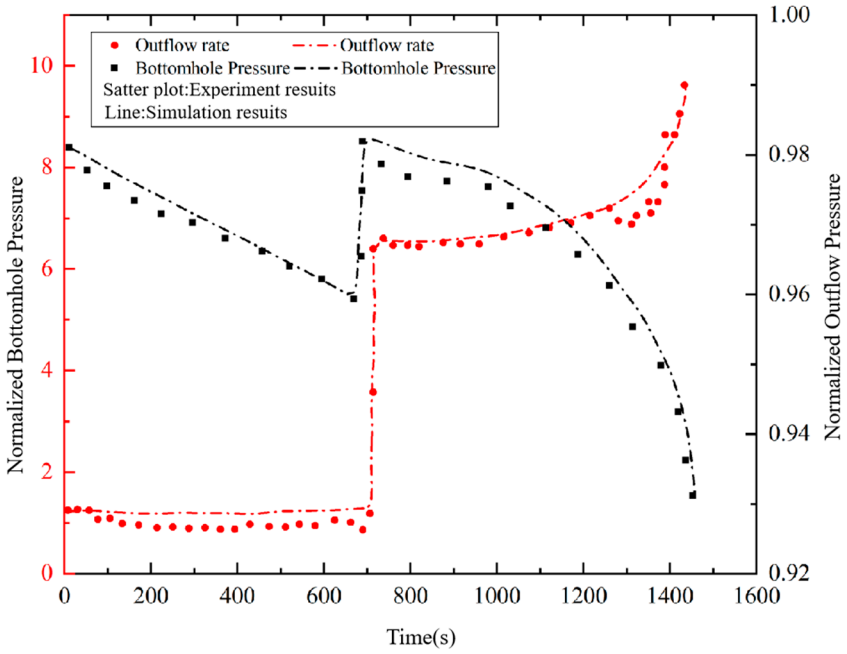


Figure 6. Comparison between experimental data and model calculation results.

3. Characteristics of Three-Phase Flow After Gas Intrusion in Hydrate Drilling

3.1. Three-Phase Flow Characteristics in Typical Well Sections

Figure 7 is a schematic diagram of the volume fraction of cuttings at the stable cross-sections of the vertical section, build-up section, and horizontal section during gas invasion. The colors represent the volume fraction of cuttings. The maximum filling volume of the volume fraction is 0.63. Red indicates that the cuttings are at the maximum volume fraction, and dark blue indicates no cuttings. Figures 8–10 are similar. It can be seen that the gas invasion has no significant impact on the cuttings' carrying capacity in the vertical section and the holding angle section. However, for the horizontal section, the apparent viscosity of the drilling fluid decreases due to gas invasion, and the cuttings' carrying capacity decreases, which will cause the thickness of the cutting bed on the lower wellbore wall to increase. This result is similar to the simulation results of Liu et al. [20].

When gas invades the wellbore, in the initial stage, a water hammer effect is formed, which causes the pressure in the wellbore annulus to rise. As the gas invasion time progresses, the annulus pressure fluctuates and decreases. After reaching stability, the pressure gradient in the wellbore annulus gradually stabilizes [21]. Compared to the situation before gas invasion, as shown in Table 2, the pressure in the vertical section decreases by 1% year-on-year, the pressure in the build-up section decreases by 10% year-on-year, and the pressure in the horizontal section decreases by 58.5 Pa. It can be seen that when the gas invasion is stable, the annulus pressure in the horizontal section decreases. For the vertical and build-up sections, the farther away from the ground, the greater the year-on-year decrease in the pressure gradient.

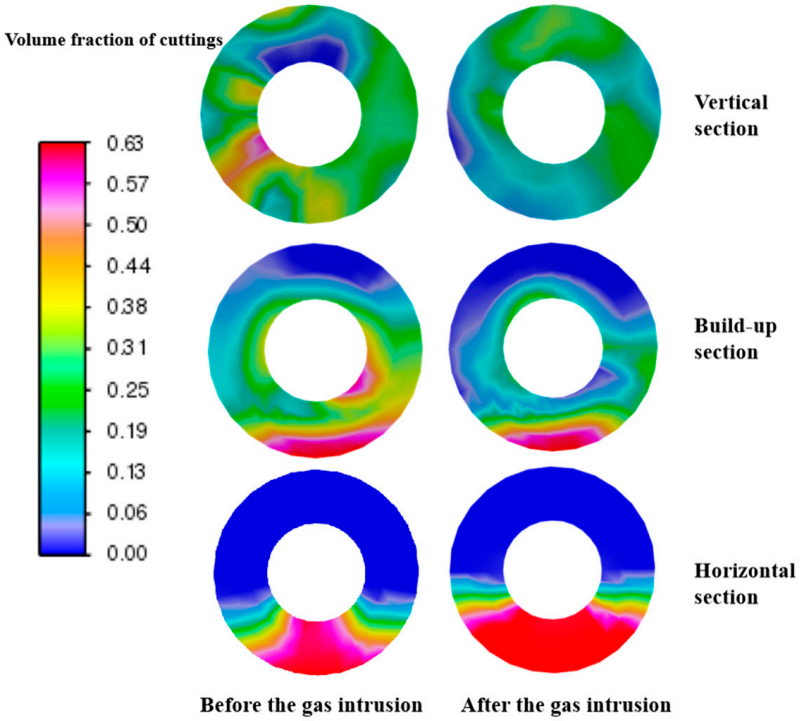


Figure 7. Schematic diagram of the volume fraction of cuttings at the stable cross-sections of the vertical section, build-up section, and horizontal section during gas invasion.

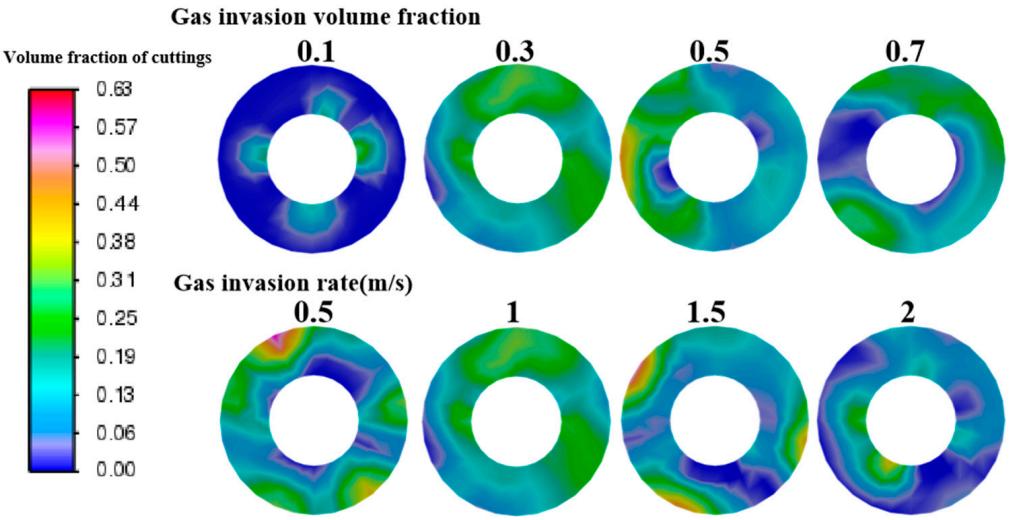


Figure 8. Schematic diagrams of gas and cuttings in the vertical section under different invasion amounts.

Table 2. Pressure gradient changes in each well section before and after gas invasion.

	Before Invasion	After Invasion
Pressure Gradient Variation in Vertical Section	1.15042×10^{-2} MPa	1.1378×10^{-2} MPa
Pressure Gradient Variation in Build-up Section	5.04×10^{-3} MPa	4.4852×10^{-3} MPa
Pressure Variation in Horizontal Section	1.4848375 MPa	1.4847772 MPa

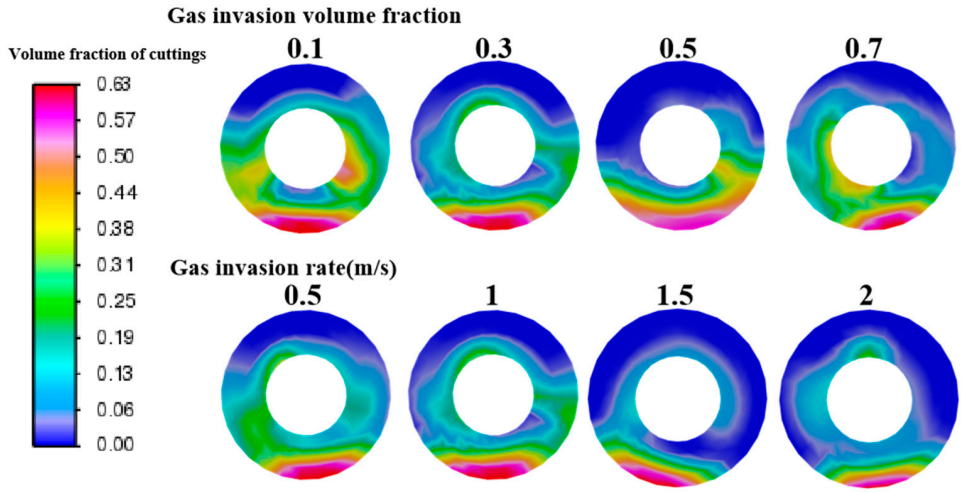


Figure 9. Schematic diagrams of cuttings in the build-up section under different invasion amounts.

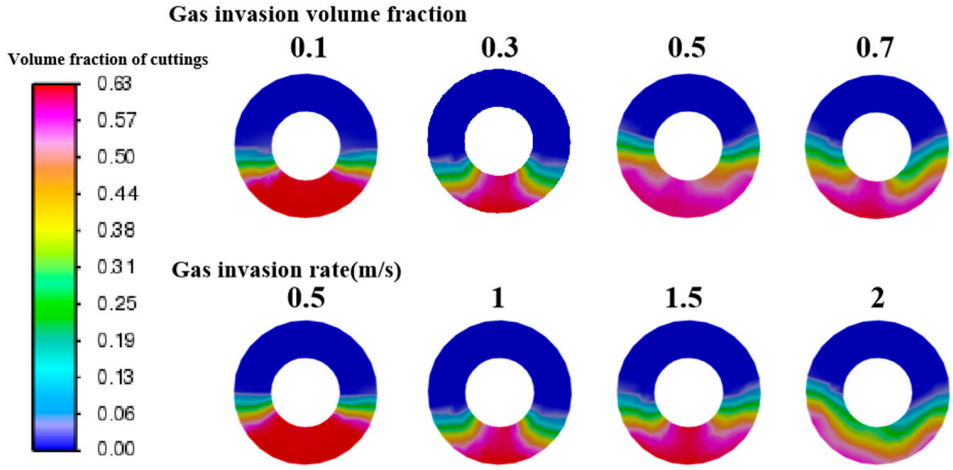


Figure 10. Schematic diagrams of cuttings in the horizontal section under different invasion volumes.

3.2. Cutting Transport Under Different Gas Intrusion Volumes

As the amount of gas invasion increases, the gas in the wellbore annulus gradually transitions from bubble flow to annular flow [22]. As shown in Figure 8, in the vertical section, when the gas invasion volume fraction is 0.1, the distribution of cuttings in the wellbore is mainly concentrated around the drill pipe. When the gas invasion volume fraction increases to 0.3, the gas is in a foam flow state. Due to the enhanced disturbance generated by the rising gas, more turbulence is created in the wellbore, and the distribution of cuttings begins to show a tendency to disperse. When the gas invasion volume fraction reaches 0.5 and 0.7, the gas forms a stable annular flow or slug flow in the wellbore, causing the cuttings to distribute along the wellbore wall. The gas velocity has a more significant impact on the cuttings in the vertical wellbore. As shown in Figure 8, with the increase in the invasion velocity, the gas can quickly reach the slug flow and annular flow patterns, generating a greater lift force on the cuttings and promoting the upward return of the cuttings in the vertical wellbore.

For the build-up section, as shown in Figure 9, with the increase in the gas volume fraction, the gas generates a lift force on the cuttings, causing the cuttings to roll and slide, thus reducing the thickness of the cutting bed. The gas velocity has an even more significant impact on the cutting bed because the lift force generated by the gas increases as the gas invasion velocity increases. In the horizontal section, with the increase in the gas invasion amount, the cuttings in the horizontal section are squeezed and returned along the lower wellbore wall. The gas invasion in the horizontal section reduces the viscosity of the

drilling fluid. However, the increase in the invasion amount will cause the cuttings to slide and roll, promoting the upward return of the cuttings. Therefore, although gas invasion reduces the viscosity of the drilling fluid, it more often promotes the upward return of the cuttings. Meanwhile, the gas invasion velocity has a greater impact on the vertical section, build-up section, and horizontal section compared to the invasion volume fraction. The most crucial factor affecting the invasion velocity is the pressure difference between the formation pressure and the bottom-hole pressure. The larger the pressure difference, the greater the invasion velocity. In engineering, this can be artificially adjusted to control the bottom-hole pressure by adjusting the density of the drilling fluid.

3.3. Wellbore Pressure Variation Characteristics Under Different Gas Intrusion Volumes

The pressure change characteristics in the vertical section, build-up section, and horizontal section of the wellbore during stable gas invasion are all different. As shown in Figure 11, since water-based drilling fluid is used in this study, gas cannot dissolve in the drilling fluid. The larger the amount of gas invading the vertical wellbore, the higher the gas content in the wellbore. The decrease in the pressure gradient will lead to further aggravation of the gas invasion, forming a vicious cycle. If no measures are taken, it may even lead to a blowout accident. The impact on the pressure gradient in the build-up section is relatively small. This is because the gas encounters relatively greater resistance during its upward movement in the annulus. Its upward velocity and the degree of disturbance to the annulus fluid are relatively weakened compared to those in the vertical section. Therefore, the change in the wellbore annulus pressure gradient is not as obvious as that in the vertical section. For the horizontal section, combined with the simulation research of Su et al. [23], as the horizontal section is at the bottom of the well, when gas initially invades the bottom of the well, the displacement at the wellhead remains basically unchanged, and the invaded gas cannot be discharged in a timely manner. At this time, the bottom-hole pressure will increase sharply with the increase in the gas invasion amount, resulting in a large pressure difference between the gas-invaded area and the non-gas-invaded area, thus exacerbating the gas invasion. Although gas invasion can promote the migration of cuttings to a certain extent, if not stopped and intervened in a timely manner, it is very likely to cause a blowout accident as the invasion amount increases. Therefore, when the amount of gas or cuttings returning upward in the vertical section is detected to be abnormal, well killing should be carried out in a timely manner.

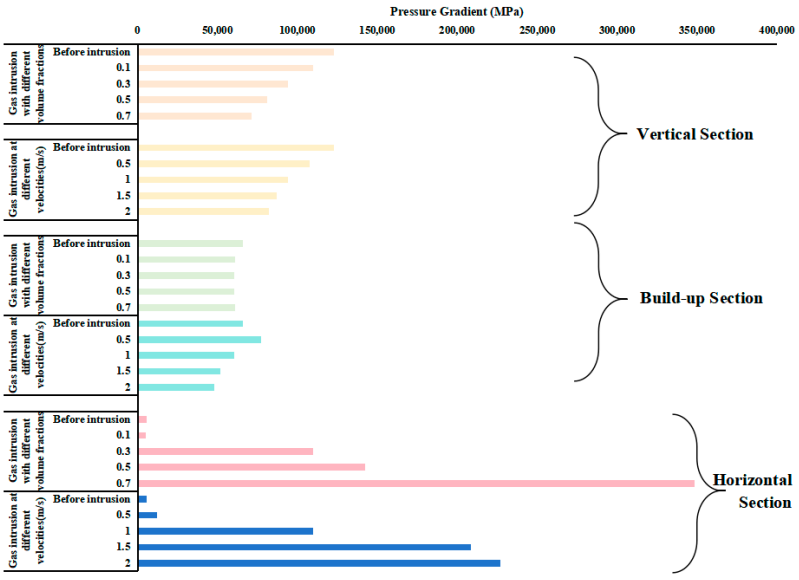


Figure 11. Pressure gradient variation trend in the vertical wellbore section.

3.4. Flow Characteristics Under Different Drilling Fluid Densities

As can be seen from the above analysis, the changes in the pressure gradient in the vertical section and the horizontal section are more significant. When the gas invasion is stable, both the pressure and the pressure gradient in the wellbore annulus show a decreasing trend compared to those before the gas invasion. At this time, if measures are not taken in a timely manner, it is very likely to cause wellbore collapse or blowout accidents. In engineering, generally, the method of increasing the density of the drilling fluid for well killing is adopted to prevent further losses [24]. This subsection selects two sets of gas intrusion volumes to simulate and calculate the pressure gradient under different drilling fluid densities, as shown in Figure 12, which depicts the pressure gradient variation in the vertical section under different drilling fluid densities. When the natural gas intrusion volume is 0.5 m/s, with a gas intrusion volume fraction of 0.17, increasing the drilling fluid density to 1150 kg/m^3 can control the well; when the natural gas intrusion volume is 0.5 m/s, with a gas volume fraction of 0.68, increasing the drilling fluid density to 1452 kg/m^3 can control the well. There is a high linear correlation between pressure gradient and drilling fluid density during gas intrusion, with correlation indices above 0.9. The relationship between pressure gradient and drilling fluid density under different gas intrusion volumes only differs in intercept, ideally increasing proportionally with gas intrusion volume. When increasing drilling fluid density, the horizontal bottom-hole pressure gradually fluctuates upward, with a fluctuation range of less than 0.1 MPa, as shown in Figure 13, having minimal impact on bottom-hole stability. Therefore, for the drilling fluid, cutting parameters, and wellbore conditions used in this simulation, when the gas intrusion volume fraction in the wellbore is less than 20%, to prevent further gas intrusion, increasing the drilling fluid density by 100 kg/m^3 can control the well. Subsequently, for every 10% increase in the gas volume fraction in the wellbore, the drilling fluid density should be increased by 50 kg/m^3. For other drilling fluids and well conditions in engineering, calculations and experiments should be conducted in advance to determine the drilling fluid density for well control under different gas intrusion volumes.

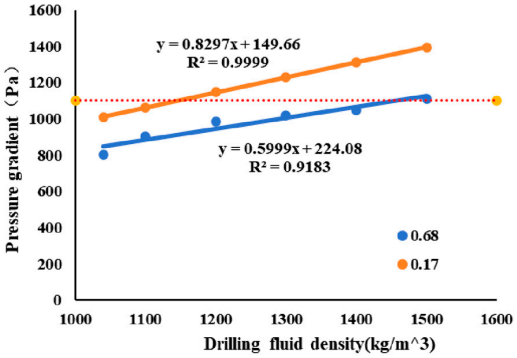


Figure 12. Pressure gradient in the vertical section varies with changes in the drilling fluid density.

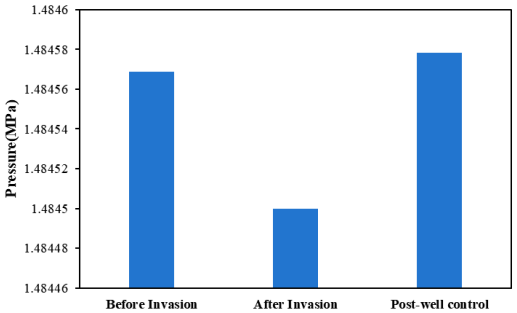


Figure 13. When the influx rate is 0.5 m/s, the pressure changes at a certain moment in the horizontal well section after well control.

4. Conclusions and Recommendations

Aiming at the gas invasion problem during subsea hydrate drilling, a multiphase fluid CFD simulation method based on the Eulerian model was optimized. The complex annulus gas–liquid–solid three-phase flow based on particle dynamics was simulated with the help of Fluent 23R1 software, providing a reference for the subsequent drilling design of hydrate reservoirs.

(1) The results show that the gas invasion velocity has a more significant impact on the migration of cuttings in different well sections compared to the gas invasion volume fraction. A faster invasion velocity accelerates the upward return of cuttings in the wellbore annulus.
(2) When gas invasion occurs, the pressure gradient changes in the vertical section and the horizontal section are significant.
(3) When gas invasion is detected at the wellhead, well killing should be carried out promptly to prevent further aggravation of gas invasion. There is a high linear correlation between the pressure gradient and the density of water-based drilling fluid during gas invasion. Taking the case in this paper as an example, when the volume fraction of gas at the outlet is detected to be less than 20%, the density of the drilling fluid should be increased by 100 kg/m^3. If it is greater than 20%, for every 10% increase in the gas volume fraction, the density of the drilling fluid should be increased by 50 kg/m^3.

The simulation in this study consumed a significant amount of time. In the future, machine learning (ML) techniques/algorithms such as neural networks or random forests can be adopted. This approach can better understand the modeling of large-scale simulation datasets to identify hidden patterns and inform decision-making. Primarily, it can recognize phase behavior patterns and predict potential outcomes under different operating conditions.

Author Contributions: Validation, J.W.; Formal analysis, S.D.; Resources, W.G.; Data curation, X.W.; Writing—original draft, J.D.; Visualization, B.L.; Supervision, C.L. All authors have read and agreed to the published version of the manuscript.

Funding: This research was funded by the National Key R&D Program of China (Grant No. 2021YFB3401400) and the Projects of the Scientific Research and Technological Development of CNPC (Grant No. 2022DQ0518).

Data Availability Statement: The data generated in this study are available upon request from the corresponding author.

Conflicts of Interest: Author Bin Li was employed by Guangzhou Marine Geological Survey. Authors Jianwei Di and Xiaodong Wu were employed by CNPC Offshore Engineering Co., Ltd. The remaining authors declare that the research was conducted in the absence of any commercial or financial relationships that could be construed as a potential conflict of interest.

References

1. Ye, J.; Qin, X.; Xie, W.; Lu, H.; Ma, B.; Qiu, H.; Liang, J.; Lu, J.; Kuang, Z.; Lu, C.; et al. Main progress of the second gas hydrate trial production in the South China Sea. *Geol. China* **2020**, *47*, 557–568.
2. Sun, B.; Fu, W.; Wang, N.; Wang, Z.; Gao, Y. Multiphase flow modeling of gas intrusion in oil-based drilling mud. *J. Pet. Sci. Eng.* **2019**, *174*, 1142–1151. [CrossRef]
3. Lv, X.; Xu, K.; Liu, Y.; Wang, C.S.; Peng, M.G.; Du, H.; Chen, S.C.; Ma, Q.; Zhou, S.; Song, S. Numerical simulation analysis of stable flow of hydrate slurry in gas-liquid-solid multiphase flow. *Ocean Eng.* **2024**, *300*, 117336. [CrossRef]
4. Pang, B.; Wang, S.; Wang, Q.; Yang, K.; Lu, H.; Hassan, M.; Jiang, X. Numerical prediction of cuttings transport behavior in well drilling using kinetic theory of granular flow. *J. Pet. Sci. Eng.* **2018**, *161*, 190–203. [CrossRef]

5. Wei, N.; Sun, W.; Meng, Y.; Zhou, S.; Li, G.; Guo, P.; Dong, K.; Li, Q. Sensitivity analysis of multiphase flow in annulus during drilling of marine natural gas hydrate reservoirs. *J. Nat. Gas Sci. Eng.* **2016**, *36*, 692–707. [CrossRef]
6. Epelle Emmanuel, I.; Gerogiorgis Dimitrios, I. Drill cuttings transport and deposition in complex annular geometries of deviated oil and gas wells: A multiphase flow analysis of positional variability. *Chem. Eng. Res. Des.* **2019**, *151*, 214–230. [CrossRef]
7. Salubi, V.; Mahon, R.; Oluyemi, G.; Oyeneyin, B. Effect of two-phase gas-liquid flow patterns on cuttings transport efficiency. *J. Pet. Sci. Eng.* **2022**, *208*, 109281. [CrossRef]
8. Shen, Z.; Wang, D.; Zheng, T. Numerical simulations of the synthetic processes and consequences of secondary hydrates during depressurization of a horizontal well in the hydrates production. *Energy* **2023**, *263*, 125675. [CrossRef]
9. Ye, J.; Qin, X.; Xie, W.; Lu, H.L.; Ma, B.J.; Qiu, H.J.; Liang, J.; Lu, J.; Kuang, Z.; Lu, C.; et al. The second natural gas hydrate production test in the South China Sea. *China Geol.* **2020**, *3*, 197–209. [CrossRef]
10. Yan, K.; Che, D. A coupled model for simulation of the gas–liquid two-phase flow with complex flow patterns. *Int. J. Multiph. Flow* **2010**, *36*, 333–348. [CrossRef]
11. Lee, D.; Sung, W. Least squares based cell-to-cell interference cancelation technique for multi-level cell NAND flash memory. In Proceedings of the 2012 IEEE International Conference on Acoustics, Speech and Signal Processing (ICASSP), Kyoto, Japan, 25–30 March 2012; IEEE: Piscataway, NJ, USA, 2012; pp. 1601–1604.
12. Agarwal, A.; Biegler, L.T.; Zitney, S.E. Simulation and optimization of pressure swing adsorption systems using reduced-order modeling. *Ind. Eng. Chem. Res.* **2009**, *48*, 2327–2343. [CrossRef]
13. Ning, A. Using blade element momentum methods with gradient-based design optimization. *Struct. Multidiscip. Optim.* **2021**, *64*, 991–1014. [CrossRef]
14. Na, K.; Kim, J. Volume fraction optimization of functionally graded composite panels for stress reduction and critical temperature. *Finite Elem. Anal. Des.* **2009**, *45*, 845–851. [CrossRef]
15. Chakchak, S.; Hidouri, A.; Ghabi, A.; Chrigui, M.; Boushaki, T. Numerical Study of Turbulent Swirling Diffusion Flame Under Lean and Rich Conditions Using Turbulence Realizable k-epsilon Model. *Combust. Sci. Technol.* **2023**, *195*, 1461–1482. [CrossRef]
16. Rodi, W. Experience with two-layer models combining the k-epsilon model with a one-equation model near the wall. In Proceedings of the 29th Aerospace Sciences Meeting, Reno, NV, USA, 7–10 January 1991; p. 216.
17. Gong, W.; Li, C.; Deng, S.; Ren, Q.; Xiao, Y.; Chen, H. Simulation study of two-phase flow in branched horizontal wells. *Mar. Georesources Geotechnol.* **2024**, 1–13. [CrossRef]
18. Elqotbi, M.; Vlaev, S.D.; Montastruc, L.; Nikov, I. CFD modelling of two-phase stirred bioreaction systems by segregated solution of the Euler–Euler model. *Comput. Chem. Eng.* **2013**, *48*, 113–120. [CrossRef]
19. Rommetveit, R.; Vefring, E.H. Comparison of results from an advanced gas kick simulator with surface and downhole data from full scale gas kick experiments in an inclined well. In Proceedings of the SPE Annual Technical Conference and Exhibition, Dallas, TX, USA, 6–9 October 1991; SPE: Kuala Lumpur, Malaysia, 1991.
20. He, M.; Liu, G.; Li, J.; Li, M.; Wang, H. The Research of Cuttings Migration during Gas Invasion. *Sci. Technol. Eng.* **2014**, *14*, 27–31.
21. Liu, F.; Cheng, C.; Qiao, S.; Xing, X.; Wu, Y.; Yang, H. Transient Variation of Annular Pressure at the Initial Stage of Gas Influx. *Drill. Prod. Technol.* **2022**, *45*, 1–7.
22. Liu, D.; Yang, Q.; Zhang, W.; Xue, X. Analysis of flow characteristics of gas-liquid two-phase flow in horizontal Wells. *China Pet. Chem. Stand. Qual.* **2023**, *43*, 81–84.
23. Su, Y.; Ma, H.; Guo, J.; Shen, X.; Yang, Z.; Wu, J. The behaviors of gas-liquid two-phase flow under gas kick during horizontal drilling with oil-based muds. *Petroleum* **2024**, *10*, 49–67. [CrossRef]
24. Feng, J.; Fu, J.; Chen, P.; Liu, Z.; Wei, H. Predicting pressure behavior during dynamic kill drilling with a two-phase flow. *J. Nat. Gas Sci. Eng.* **2015**, *22*, 591–597. [CrossRef]

Disclaimer/Publisher's Note: The statements, opinions and data contained in all publications are solely those of the individual author(s) and contributor(s) and not of MDPI and/or the editor(s). MDPI and/or the editor(s) disclaim responsibility for any injury to people or property resulting from any ideas, methods, instructions or products referred to in the content.